Journal of Geoscience and Environment Protection, 2026, 14(6), 23-40
https://www.scirp.org/journal/gep
ISSN Online: 2327-4344
ISSN Print: 2327-4336

The Formation of Mantle Melt and the Causes of Its Heterogeneous Distribution

Mengke Zhang, Guowen Zhang*

Wuhan Neutrino Science & Technology Co., Ltd., Wuhan, China
Email: *gwz1000@sina.com

How to cite this paper: Zhang, M. K., & Zhang, G. W. (2026). The Formation of Mantle Melt and the Causes of Its Heterogeneous Distribution. *Journal of Geoscience and Environment Protection, 14,* 23-40.
https://doi.org/10.4236/gep.2026.146002

Received: May 8, 2026
Accepted: June 12, 2026
Published: June 15, 2026

Abstract

Geophysical observations indicate that the upper mantle contains a small amount of melt, which is distributed unevenly. Overall, the oceanic mantle contains significantly more melt than the continental mantle, and the asthenosphere contains the most melt, whether beneath oceans or continents. Current theories of melt formation cannot explain this uneven distribution of melt within the mantle. Here, based on the latest research findings regarding neutrino oscillation-induced radioactive decay and mantle melt formation, we further investigate the influence of Earth's material density on atmospheric neutrino oscillations. We analyze the necessary conditions for atmospheric neutrinos to generate Mikheyev-Smirnov-Wolfenstein (MSW) resonance within the Earth's interior, and discuss the heat generation from MSW resonance-induced radioactive decay, as well as the formation and distribution of the melt. The results indicate that the necessary conditions for atmospheric neutrinos to generate MSW resonance within the Earth are: a constant material density and a width (or thickness) exceeding a certain threshold. The composition of the crust is complex, with significant fluctuations in density; there are no material layers with a width exceeding the threshold and a constant density, making it difficult to form MSW resonance. In contrast, mantle material is relatively homogeneous and possesses a certain degree of plasticity, allowing for creep. Its density varies uniformly, and within relatively thin layers, the density remains essentially constant, satisfying the conditions required for the formation of MSW resonance. Therefore, MSW resonance can occur in the mantle, inducing radioactive decay and heat generation, and producing melt. At the same time, we demonstrate that due to tectonic stresses at the Earth's surface, mantle melt migrating upward converges beneath low-stress arched structures (mountain ranges), thereby forming a laterally inhomogeneous distribution.

Keywords

Atmospheric Neutrinos, Neutrino Oscillation-Induced Radioactive Decay,

Melt Formation, Arched Structure, Distribution of Mantle Melt

1. Introduction

The presence of small amounts of melt in the mantle and asthenosphere has been confirmed by geophysical observations and is widely accepted (Zohoori & Spetzler, 1970; Mierdel et al., 2007; Chantel et al., 2016; Debayle et al., 2020; Liu & Yang, 2024). Experiments have shown that shear wave velocity (Vs) is closely related to temperature, composition, and melt content, whereas shear wave attenuation (Qs) is largely unaffected by chemical composition but is strongly influenced by temperature, varying in an exponential relationship with temperature. Therefore, by comparing observations of Vs and Qs, it is possible to estimate the melt content in the mantle and asthenosphere (Selway & O'Donnell, 2019). Debayle et al. (2020) based on extensive Rayleigh surface wave data recorded at relevant stations, utilized seismic surface wave tomography methods. By establishing global models of shear wave velocity (DR2020s) and shear wave attenuation (QsASDR17) at different depths in the upper mantle, and combining these with experimental results and corresponding simulations of how Vs and Qs vary with temperature, pressure, and melt content, they calculated the melt content at various depths within the upper mantle. The results indicate that melt is generally present in the Low-Velocity Zone (LVZ) at depths of 150 - 200 km within the oceanic asthenosphere, with a melt fraction below 0.3%. However, beneath mid-ocean ridges, major hotspots, and post-arc regions near the Pacific Ocean at depths of 100 - 200 km, the melt fraction exceeds 0.3% and can reach 0.7%; Small amounts of melt are present at a depth of 300 km beneath tectonically active regions on continents, such as the East African Rift Valley, the Qinghai-Xizang Plateau, Balleny Island in Antarctica, and the western United States; virtually no melt was detected at a depth of 350 km in the global mantle (**Figure 1**). These results indicate that the distribution of mantle melt is characterized by heterogeneity. Overall, melt is concentrated in the upper mantle, with the highest concentrations found in the asthenosphere. Melt is more abundant beneath mountain ranges (including mid-ocean ridges) than in other regions, and the upper mantle and asthenosphere of the oceans are more enriched in melt than those of the continents.

For mantle rocks to melt, the temperature must exceed their solidus. There are two ways to achieve this: first, by heating the rocks to a temperature above their solidus; second, by lowering the solidus temperature of the rocks at a constant temperature (e.g., by introducing volatiles or reducing pressure). To date, the primary sources of energy input into the mantle are radioactive materials (The KamLAND Collaboration, 2011) and mantle plumes (Choi, 2013; Koppers et al., 2021). However, radioactive materials are distributed relatively uniformly, which cannot explain the heterogeneity of mantle melts, while mantle plumes occur only at a few hotspots and cannot provide energy for the formation of asthenospheric

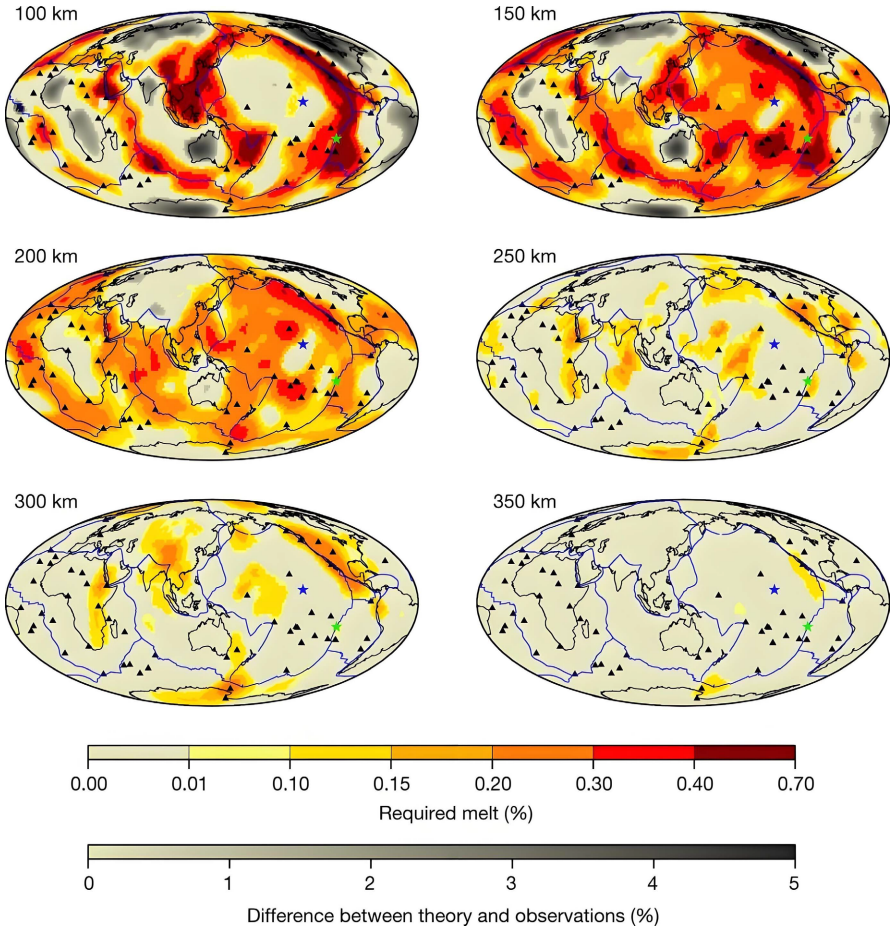

Figure 1. Melt contents at different depths in the upper mantle. The images are from Debayle et al. (2020).

melts far from these hotspots. Therefore, it is generally believed that the primary cause of mantle melt formation is the decompression of ascending mantle material, or the incorporation of water, which lowers the melting point of the rock, leading to the melting of a portion of the material (Lambert & Wyllie, 1970; Gu et al., 2001; Mierdel et al., 2007; Xia et al., 2022; Niu, 2023). The mantle is generally dry, and water is typically introduced only through plate subduction (Xia et al., 2022). However, subduction and mantle upwelling occur only in localized regions, which contradicts the global distribution of the melt-rich asthenosphere. Therefore, subduction-induced water injection and mantle upwelling cannot fully explain the formation of mantle and asthenospheric melts. Based on estimates of the geothermal gradient, the temperature of the asthenosphere is insufficient to cause the rocks in that region to melt. Therefore, without the addition of volatiles or external energy, the heat provided solely by the geothermal gradient is insufficient to cause partial melting of the material in this region. Consequently, the mechanism responsible for the partial melting of the mantle and asthenosphere remains a subject of debate (Zhang, 1999; Gu et al., 2001; Du, 2005; Mierdel et al., 2007; Chen, 2013; Debayle et al., 2020). Furthermore, research indicates (Smye & Kele-

men, 2025) that the formation of stable cratonic crust requires an ultra-high-temperature environment to transport radioactive elements such as U and Th into the upper crust. Since mantle upwelling alone cannot generate such ultra-high temperatures, what mechanisms could produce these ultra-high temperatures in the mantle and lower crust? This question requires further investigation.

Recently, Zhang & Zhang (2024a) proposed that heat generated by neutrino-induced radioactive decay provides the energy for the formation of mantle and asthenosphere melts. Using this energy as a driving force, they explained the formation of a series of tectonic features, including the asthenosphere, the lithosphere-asthenosphere boundary (LAB), paired metamorphic belts, new oceanic crust and a strip-shaped magnetic anomaly on the mid-ocean ridges (Zhang & Zhang, 2024b, 2025a, 2025b). However, they did not provide a detailed explanation for issues such as the non-uniform lateral distribution of melts in the upper mantle and asthenosphere.

In this work, we extend the research of Zhang & Zhang (2024b, 2025a) to discuss the necessary conditions for atmospheric neutrino oscillations to generate Mikheyev-Smirnov-Wolfenstein (MSW) resonance (Wolfenstein, 1978; Mikheyev & Smirnov, 1986, 1989) resonance within the Earth's interior, analyzed the stratigraphic layers and regions in the Earth's interior that satisfy the requirements for MSW resonance, and provided a satisfactory explanation for issues such as the non-uniform distribution of mantle melt.

2. Method

Based on the MSW resonance theory of neutrino oscillations established by Wolfenstein (1978) and Mikheyev & Smirnov (1986, 1989), and incorporating the latest research findings by Zhang & Zhang (2024a, 2024b) on neutrino oscillation-induced radioactive decay and magma formation, this study analyzes the formation of MSW resonance and the generation of melt by atmospheric neutrinos within the Earth's interior. By comparing these findings with geophysical observation results, this study proposes the necessary conditions for the formation of MSW resonance and the generation of melt. Additionally, based on the surface arching effect (Zhang & Zhang, 2024c), we discuss the dynamics and global distribution of mantle melt migration. The Earth density data used in this paper are derived from the PREM (Preliminary Reference Earth Model) (Dziewonski & Anderson, 1981), while the energy spectrum data for atmospheric neutrinos are taken from Honda & Kajita (1995) and Gaisser & Honda (2002).

2.1. MSW Resonance of Atmospheric Neutrinos in the Earth's Interior

Wolfenstein (1978) was the first to establish the evolution equations for neutrinos in a medium and studied the matter effects of neutrino oscillations. Building on Wolfenstein's evolution equations for neutrinos in a medium, Mikheyev & Smirnov (1986, 1989) further derived the existence of resonance phenomena in neutrinos

propagating through matter, known as the MSW mechanism. For simplicity, we will use the two-flavor neutrino oscillation $\nu_e \leftrightarrow \nu_\mu$ as an example to provide a brief explanation. Neutrino conversion can be described using the instantaneous eigenstates ν_{1m} and ν_{2m} of the Hamiltonian in matter. If an arbitrary neutrino state is represented as $|\nu\rangle = \psi_{1m}|\nu_{1m}\rangle + \psi_{2m}|\nu_{2m}\rangle$, then the evolution equation for neutrinos propagating in matter can be written in terms of (ν_{1m}, ν_{2m}) (de Holanda et al., 2004):

$$i\frac{\mathrm{d}}{\mathrm{d}t}\begin{pmatrix}\psi_{1m}\\ \psi_{2m}\end{pmatrix} = \begin{pmatrix}-\dfrac{\Delta m_m^2}{4E} & -i\dfrac{\mathrm{d}\theta_m}{\mathrm{d}\chi}\\ i\dfrac{\mathrm{d}\theta_m}{\mathrm{d}\chi} & \dfrac{\Delta m_m^2}{4E}\end{pmatrix}\begin{pmatrix}\psi_{1m}\\ \psi_{2m}\end{pmatrix} \tag{1}$$

In the above equation, θ_m is referred to as the matter effect mixing angle, and Δm_m^2 is the difference in effective mass squared; their relationships with the other parameters are as follows:

$$\Delta m_m^2 = \sqrt{\left(\Delta m^2\cos 2\theta - A_{CC}\right)^2 + \left(\Delta m^2 \sin 2\theta\right)^2} \tag{2}$$

$$\frac{\mathrm{d}\theta_m}{\mathrm{d}\chi} = \frac{1}{2}\cdot\frac{\sin 2\theta_m}{\Delta m_m^2}\frac{\mathrm{d}A_{CC}}{\mathrm{d}\chi} \tag{3}$$

In Equations (2) and (3) above, E is the energy of the neutrino, θ is the mixing angle in vacuum, $\Delta m^2 = \left|m_2^2 - m_1^2\right|$ is the difference in the squares of the masses of the two mass eigenstates, and $A_{CC} \equiv 2EV_{CC} = 2\sqrt{2}EG_F N_e(\chi)$ (where G_F is the Fermi constant, $N_e(\chi)$ is the electron number density in the medium, and V_{CC} is the effective potential).

If the medium density is constant, solving the neutrino evolution equation yields the conversion probability after the neutrino has traveled a distance L:

$$P_{\nu_e\to\nu_\mu} = \sin^2 2\theta_m \sin^2\left(\frac{\Delta m_m^2 L}{4E}\right) \tag{4}$$

Neutrinos enter resonance when the following condition is satisfied:

$$N_e(\chi) = \frac{\Delta m^2\cos 2\theta}{2\sqrt{2}G_F E} \tag{5}$$

At resonance, the mixing of the two neutrino flavors reaches a maximum, and neutrino oscillations are enhanced. This is the MSW mechanism.

2.2. Atmospheric Neutrino Oscillation-Induced Radioactive Decay and Mantle Melt Formation

As is well known, resonance is a form of forced vibration triggered by external energy, which can have a highly destructive effect on fragile systems. After studying the MSW mechanism, Zhang & Zhang (2024a) further pointed out that this mechanism is, in fact, a typical physical resonance formed between neutrinos and the medium. While it strongly influences neutrino oscillation behavior (increasing flavor mixing), it also exerts a certain influence on the nucleons in the me-

dium, exciting them into excited states. This leads to further destabilization of unstable radioactive nucleons, thereby increasing their probability of decay (**Figure 2**) (Zhang & Zhang, 2024b). Since radioactive decay involves quantum tunneling effects (Gurney & Condon, 1991) and quantum transitions (Fermi, 1934), it is extremely sensitive to energy; even minute energy perturbations can cause decay rates to change exponentially.

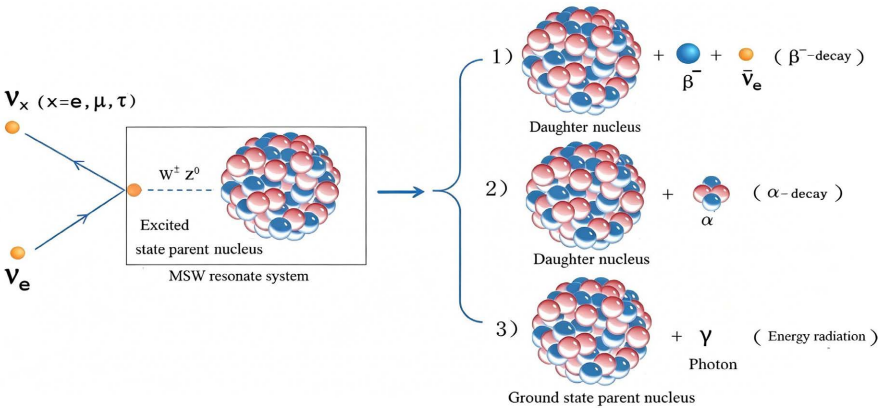

Figure 2. Neutrino oscillations perturb radioactive nuclei to decay in an excited state. This image is quoted from Zhang & Zhang (2026).

Atmospheric neutrinos, produced by the decay of mesons generated through the interaction of cosmic rays with atmospheric matter, are constantly passing through our planet (Honda & Kajita, 1995; Kajita, 2010). The Earth contains abundant radioactive elements, with a density ranging from 1 to 13 g/cm^3 from the oceans to the Earth's core (Dziewonski & Anderson, 1981). The energies of atmospheric neutrinos are concentrated in the range of 0.1 - 10^4 GeV (Honda & Kajita, 1995; Gaisser & Honda, 2002; Kajita, 2010). Based on the conditions for MSW resonance, atmospheric neutrinos match the density of Earth's matter over a wide range, enabling them to form MSW resonance with Earth's matter in various layers. During resonance, the energy of atmospheric neutrinos can be expressed as (Upadhyay et al., 2023):

$$E_{res} = \frac{\Delta m^2 \cos 2\theta}{2\sqrt{2} G_F N_e} \approx \frac{\Delta m_{31}^2 \left[\mathrm{eV}^2\right] \cos 2\theta_{13}}{7.6\times 10^{-14} \rho \left[\mathrm{g/cm}^3\right]} \ \mathrm{eV} \tag{6}$$

In the above equation, the relationship between N_e and the material density ρ is $N_e = Y_e \rho / m_N$, where Y_e is the electron-to-nucleon ratio (i.e., the number of electrons per nucleon), and m_N is the nucleon mass number. The values of the other relevant parameters are as follows: $\Delta m_{31}^2 = 2.49\times 10^{-14}$ eV, $\sin^2 2\theta_{13} = 0.0875$.

The average density of the upper mantle is 3.5 g/cm^3. When MSW resonance occurs in the upper mantle, the neutrino energy is:

$$E_{res}^{up} = 4.41 \ \mathrm{GeV} \left(\frac{3.5 \ \mathrm{g/cm}^3}{\rho} \right) \left(\frac{\Delta m_{31}^2}{2.4\times 10^{-3} \ \mathrm{eV}^2} \right) \cos 2\theta_{13} \tag{7}$$

The average densities of the continental crust and the Earth's core are 2.7 g/cm^3 and 10.7 g/cm^3, respectively. By the same reasoning, the energies of atmospheric neutrinos when MSW resonance occurs in the continental crust and the Earth's core can be calculated to be approximately 11.67 GeV and 2.94 GeV, respectively. These energies all fall within the energy spectrum of atmospheric neutrinos.

Calculations by Zhang & Zhang (2024b) indicate that in the upper mantle, the decay of just 3.02% of major radioactive isotopes such as uranium, thorium, and potassium is sufficient to cause melting of the upper mantle material. However, in the lower mantle, due to the scarcity of radioactive materials, the heat generated by MSW-induced radioactive decay is insufficient to cause melting. Therefore, Zhang & Zhang (2024b, 2025a) propose that the melt is primarily generated in the upper mantle, formed when atmospheric neutrinos induce radioactive decay in this region, generating heat and causing partial melting of the material. This conclusion not only agrees very well with geophysical observations (Debayle et al., 2020), but also explains the formation of tectonic and dynamic phenomena such as the asthenosphere, metamorphic belts, and earthquakes (Zhang & Zhang, 2024b, 2025a, 2025b, 2025c).

It is worth noting that, compared to mechanisms involving mantle upwelling and the injection of volatiles to form melt, the temperature of melt generated by radioactive heat produced through neutrino oscillations is primarily related to the degree of radioactive element enrichment and the intensity of neutrino oscillation perturbations. This temperature can be significantly higher than that of the surrounding environment. Such ultra-high-temperature melt can more easily extract elements such as U and Th, leading to depletion of the mantle and even the lower crust.

3. Results and Discussion

Based on the MSW resonance theory (Wolfenstein, 1978; Mikheyev & Smirnov, 1986, 1989), the mechanism of radioactive decay induced by neutrino oscillations, and the new theory of magma formation (Zhang & Zhang, 2024a, 2024b), atmospheric neutrinos should be capable of generating MSW resonance as they propagate through the crust, mantle, and core. Furthermore, since both the crust and the upper mantle are rich in radioactive materials, they should both be capable of generating melt. However, geophysical observations indicate that melt is virtually absent in the crust, and melt in the upper mantle is not widely distributed; there is more melt in the upper mantle beneath the oceans and less beneath the continents (**Figure 1**) (Debayle et al., 2020). Regarding the absence of melt in the crust, which is enriched in radioactive elements, Zhang & Zhang (2024b) previously explained that, since MSW resonance in the crust had not yet fully initiated, radioactive decay was not disturbed, and no melt was generated in the crust.

However, this explanation raises several issues: First, if atmospheric neutrinos only trigger MSW resonance upon traversing the crust to reach the mantle, does the significant difference in thickness between continental and oceanic crust im-

ply that the onset of neutrino oscillation occurs at different times in these two crustal types? Second, since the oceanic mantle contains significantly more melt than the continental mantle, does this imply that the MSW resonance generated by neutrino oscillations also differs between the oceanic and continental mantles? These questions require further analysis and a clear explanation.

3.1. Necessary Conditions for MSW Resonance and Melt Formation

In the previous section, we discussed that when neutrinos propagate through matter, resonance can occur when the electron number density of the matter matches the neutrino energy. If the vacuum mixing angle is small, then for a neutrino entering a medium from vacuum to form resonance (i.e., for mixing to reach a maximum), in addition to the neutrino energy and material density satisfying Equation (5), there is also a lower limit on the amount of matter (or width) required to complete the transition between the eigenstates $\nu_1 m$ and $\nu_2 m$ and maximize mixing. The amount of matter is characterized by the electron column density along the neutrino trajectory (Lunardini & Smirnov, 2000; Smirnov, 2005):

$$d = \int_0^l N_e(\chi)\mathrm{d}\chi \tag{8}$$

The essence of neutrino oscillation resides in the coherent scattering that takes place between neutrinos and the medium they traverse. Since the medium contains electrons (e) but no muons (μ), the scattering amplitudes for ν_e and ν_μ differ. After passing through a medium with a certain line density χ, ν_e and ν_μ develop a phase difference of 2π and start to oscillate. Therefore, the degree to which the matter effect influences neutrino oscillations depends on both the density ρ and the width χ of the medium. Equation (5) merely specifies the density condition required for resonance and does not account for the medium's width. In fact, if the material thickness (or width) is too small (i.e., the material is insufficient), resonance is unlikely to form even if the density satisfies Equation (5). This is because the mixing angle formed in the material during resonance differs significantly from that in a vacuum—namely, $\theta \neq \theta_m$. This indicates that a transition has occurred between the mass eigenstates ν_{1m} and ν_{2m} in the material, thereby leading to a change in the mixing angle. Since oscillation (or transition) is affected by matter (electron number density) and requires traversing a certain width of matter (line width) to complete, neutrinos also need a specific line width of matter to achieve mixing angle conversion and reach resonance (i.e., form maximum mixing). Given that neutrinos propagate at speeds close to the speed of light, even if the conversion of the neutrino mixing angle can be completed in 10^{-5} seconds, the width traversed by the neutrinos can still reach the kilometer scale. Thus, we derive the necessary conditions for the formation of MSW resonance: the neutrino energy and matter density must satisfy Equation (5), and the thickness of the matter layer must be no less than d_p. Once initiated, resonance can perturb the decay of radioactive nucleons; consequently, d_p also represents the

minimum width required for resonance to perturb radioactive nucleon decay.

Furthermore, the formation of a melt is subject to specific conditions. In addition to the MSW resonance between neutrinos and matter, there must be an accumulation of radioactive material within the resonance region. If radioactive material is scarce, even if MSW resonance exists and perturbs radioactive decay, the total heat generated will be insufficient to produce a melt. Therefore, the necessary conditions for melt formation are: the accumulation of radioactive elements within the region and the presence of MSW resonance.

3.2. Formation of the Oceanic and Continental Mantle Melt and the Reasons for Their Differences

Melt is virtually absent in the crust (even the small amount of melt or magma in magma chambers originates from the upper mantle). This is because the density characteristics of the crust do not satisfy the conditions for MSW resonance formation; that is, there are no rock layers with a width greater than d_p that have a constant density or a smoothly varying density. The current estimates of Earth's density are based on statistical analyses of empirical relationships between seismic waves and rock density. In reality, the density distribution in the Earth's interior is significantly influenced by temperature and material composition. However, since it is impossible to directly measure temperature and material composition within the Earth, these parameters can only be inferred from geothermal gradients and pressure; therefore, the actual density of the Earth may differ from the widely used density values (such as those in the PREM model) (Fang & Xu, 1999; Chu et al., 2021). This is particularly true of the Earth's crust, which not only exhibits temperature variations due to uneven radioactive distribution but also features a complex composition comprising rocks of varying densities, such as granite (density between 2.63 and 2.75 g/cm^3), basalt (density between 2.8 and 3.3 g/cm^3), and sedimentary rock (between 2.69 and 2.7 g/cm^3). Furthermore, these rocks are interspersed with water, petroleum, and various gases. Consequently, it is difficult to find a rock layer within the actual crust that is thousands of meters thick and has a constant density. At least, no such rock layer exists in the continental crust. Consequently, atmospheric neutrinos generally struggle to generate MSW resonance within the crust, and thus no melt is produced there. Compared to the crust, the mantle consists of relatively simple minerals and exhibits plasticity, allowing it to creep slowly. The density of the mantle varies gradually throughout, and within relatively thin layers (such as within a 10-kilometer range), the density of the material remains essentially constant (Dziewonski & Anderson, 1981), satisfying the conditions for MSW resonance. Consequently, melt can form in regions of the mantle where radioactive materials are concentrated.

Furthermore, like the oceanic mantle, the continental mantle exhibits plasticity and shows minimal variation in overall density. Within relatively thin layers, there exist rock layers with essentially constant density and a width greater than d_p, capable of generating MSW resonance and driving radiogenic heat production;

however, the amount of melt in the continental mantle is significantly less than in the oceanic mantle. This is because as one descends deeper into the Earth, the pressure on the material increases, raising the melting point and requiring more heat to melt the same amount of material. Therefore, even if MSW resonance perturbs radioactive decay to produce the same amount of heat in both the oceanic and continental mantles, the continental mantle generates far less melt than the oceanic mantle due to its higher melting point.

3.3. The Origin of the Asthenosphere and LAB

The asthenosphere is a global zone of low velocity in the upper mantle. In oceanic and continental regions, the upper boundary of the asthenosphere lies at depths of approximately 40 - 60 km and 80 - 120 km, respectively, and can reach 150 - 250 km in some ancient cratons (Sleep, 2005; Fischer et al., 2010). The origin of the asthenosphere has long been a subject of debate. These debates center on two key issues: first, whether the low-velocity zones result from partial melting or mineral hydration; and second, how the melting occurs, or where the injected water originates (Karato, 2012; Hua et al., 2023). It is currently widely accepted that partial melting is the primary factor in the formation of the asthenosphere (Chantel et al., 2016; Debayle et al., 2020; Hua et al., 2023). However, the formation mechanism of the asthenosphere melt remains controversial (Zhang, 1999; Du, 2005; Chen, 2013). The primary reason for this controversy is that no single mechanism can fully explain the global distribution of the asthenosphere melt or the depth variations between continental and oceanic regions. Clearly, based on the melt formation mechanism proposed in this paper, the melts in the asthenosphere also originate from the heat generated by radioactive decay induced by atmospheric neutrino oscillation perturbations. Why, then, is the melt content in the asthenosphere significantly higher than in other regions of the mantle? Zhang & Zhang (2024b) propose that the generation of melt by neutrino oscillations is a stochastic process that follows a normal distribution in space, with the asthenosphere being the region where melt distribution is most concentrated. However, this explanation lacks theoretical derivation and remains highly ambiguous. In fact, we can demonstrate this through direct calculations. Studies show that if 3.02% of the major radioactive isotopes in a given region of the upper mantle undergo rapid decay, it can lead to complete melting of that region (Zhang & Zhang, 2024b). Since mantle material is typically partially molten, the proportion of rapidly decaying radioactive isotopes should be less than 3.02%. Now, let us assume that neutrino oscillations disturb 1 g of mantle material at different depths, causing 2.00% of the radioactive material to decay and generate heat. According to the calculations in Zhang & Zhang (2024b), the heat generated by the complete decay of radioactive material in 1000 kg of upper mantle material can reach 1.69×10^{10} J. From this, we can estimate that the heat generated by the decay of 2.00% of the radioactive material in 1 g of mantle material is approximately 338 J. Since pressure and temperature are essentially constant in a small region, the heat Q con-

sumed by the melting of the rock can be calculated using the following formula:

$$Q = C_p M\left(T - T_0\right) + Lm \tag{9}$$

In the above equation, C_p is the specific heat capacity, M is the mass of rock as the temperature rises from T_0 to the melting point T, L is the latent heat of fusion, and m is the mass of rock that transitions from a solid to a liquid state at the melting point T.

At the top of the upper mantle (33 km below the surface, where the temperature is approximately 1000˚C and the specific heat capacity is 1000 J/kg·K), it takes approximately 300 J of heat to raise 1 g of rock from 1000˚C to its melting point of 1300˚C; the remaining 38 J can be used to melt the rock. Assuming the latent heat of fusion is 210 kJ/kg, the amount of rock melted is 0.18 g; At a depth of 100 km (i.e., the asthenosphere), since the geothermal temperature is already close to the liquidus temperature, the heat required to raise the rock to its melting point is negligible. Almost all of the injected heat is used to melt the rock. Assuming a latent heat of fusion of 600 kJ/kg, 338 J of heat can cause 0.56 g of rock to melt; At a depth of 300 km, the geothermal temperature is also close to the liquidus temperature. Assuming a latent heat of fusion of 800 kJ/kg, 338 J of heat can cause 0.42 g of rock to melt. These calculations clearly show that injecting the same amount of heat produces the most melt in the asthenosphere. This is because as depth increases, pressure rises, the liquidus temperature of minerals increases, and the latent heat of fusion increases; therefore, when the same amount of heat is injected at different depths, the amount of melt produced decreases with increasing depth; Conversely, as depth increases, temperature rises, and the gap between the rock's temperature and its liquidus temperature narrows. Therefore, when heating mantle material at different depths to induce melting, less heat is required at greater depths. In other words, as depth increases, injecting the same amount of heat produces more melt. The superposition of these two opposing trends inevitably results in a region where melt production is maximized—this region is the asthenosphere.

Apart from the asthenosphere, sporadic melt pockets are randomly distributed throughout the upper mantle; however, the amount of melt in other regions is so small that it is difficult to detect.

Melt initially forms in tiny regions where radioactive elements are relatively enriched, existing as melt pocket (Liu, 2020). As the heat generated by radioactive elements increases due to neutrino oscillation perturbations and temperatures rise, these melt pockets gradually grow and coalesce, forming larger, mobile melt bodies. These melt bodies are high in temperature and low in density, generating buoyancy. Driven by this buoyancy, the melt continuously permeates, rises, and coalesces through the interstitial spaces between mineral grains. As the ascent height increases, the temperature of the melt gradually decreases, and its viscosity increases accordingly. At the same time, the creep rate of the mantle continuously decreases. When the melt reaches the lithosphere, it is blocked by the permeability barrier at the lower boundary of the lithosphere, preventing it from continuing to

ascend through permeation. Consequently, it can only ascend and migrate along faults or fractures. Consequently, large volumes of melt become trapped at the lithosphere-asthenosphere boundary (LAB), leading to a significant increase in melt content in this region and the formation of a sharp discontinuity in seismic waves (Schmerr, 2012; Zhang & Zhang, 2024b).

Since most of the melt in the asthenosphere is locally melted, its composition retains its original characteristics, being more silicon-poor and iron-rich. In contrast, the vast majority of the melt in the LAB has migrated upward from the deep mantle (Schmerr, 2012). During this migration, due to heat loss, some ultramafic minerals in the melt crystallize out, resulting in the LAB melt being relatively silicon-rich and iron-poor (Zhang et al., 2024).

3.4. The Influence of Surface Arch Structures on the Distribution of Mantle Melt

The distribution map of upper mantle melt (**Figure 1**) compiled by Debayle et al. (2020) based on geophysical survey results shows that melt tends to accumulate beneath mid-ocean ridges, major hotspots, and back-arc regions near the Pacific Ocean, whereas very little melt is present beneath ocean basins and continents. This distribution of melt is the result of its migration under stress following its generation. In addition to buoyancy, mantle melt is also subject to tectonic stresses. Near the Earth's surface, tectonic stresses primarily originate from the arch-like structural effects formed by variations in surface topography.

In their study of the coupled evolution of basins and mountains, Zhang & Zhang (2024c) established a tectonic dynamic model of basin-mountain coupling. They proposed that the basin-mountain-basin system forms an arch-like structure, resulting in distinct stress distributions within the system. The mountain range acts as the arch, while the basins (or plains) on either side serve as the arch feet (**Figure 3**). The arch (mountain range) converts its immense gravitational force into lateral compressive stress (i.e., circumferential stress) transmitted to the basins on both sides, causing the pressure on the mountain margins and basins to be far greater than that in the interior of the mountain range. The stress difference generated by this arch-like tectonic effect provides the driving mechanism for basin subsidence and mountain uplift. The stress characteristics of an arch-like structure are as follows: under the vertical load q acting on the arch-like structure, the support points generate not only a vertical reaction force V but also a horizontal thrust H (**Figure 4**). It can be demonstrated that the lateral stress in an arch structure exceeds its vertical gravitational force (Mao et al., 2020; Zhang & Zhang, 2024c). For mountain ranges, this means that the stress on the rocks beneath the foothills (at the base of the arch) is far greater than that on the rocks in the interior of the range (directly beneath the arch). So a low stress zone was created in the belly of the mountain range.

Stresses generated by arch tectonic effects can be transmitted downward through the lithosphere into the mantle. Consequently, a low-stress zone forms in

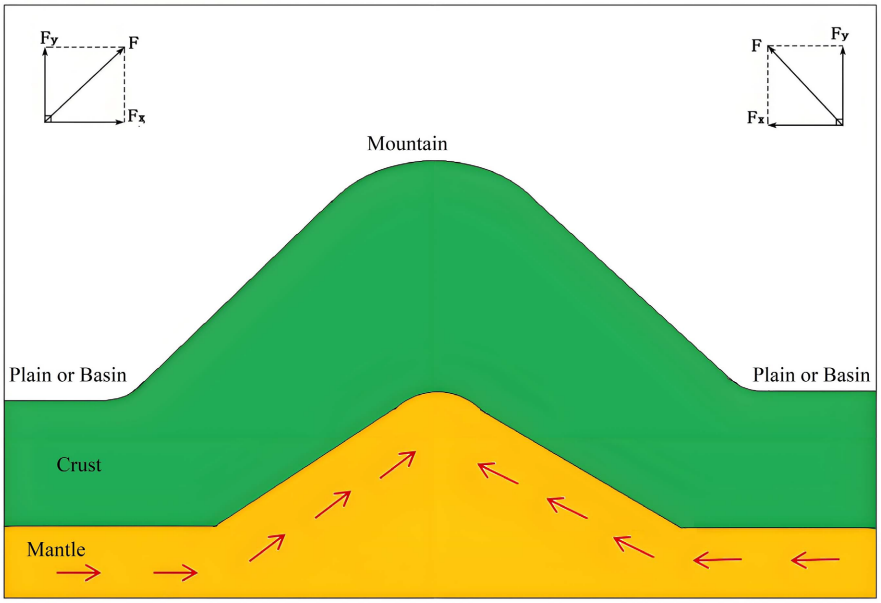

Figure 3. Schematic diagram of the basin-mountain-basin arch structure and the force and migration direction of the melt below the mountain. The arrow indicates the direction of mantle melt migration.

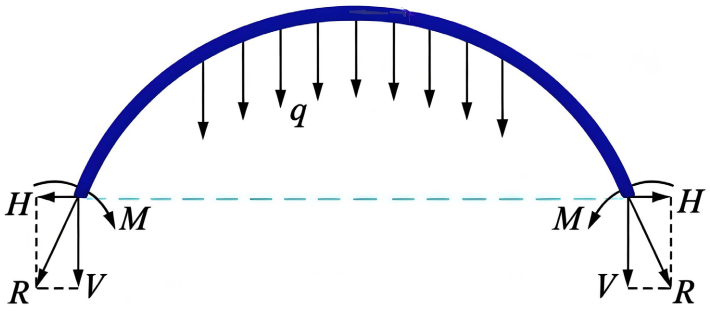

Figure 4. Stress condition of arch structure. Image quoted from Zhang & Zhang (2024c).

the mountain arc, extending from the crust to the upper mantle, while the mountain margins and the basins on either side become high-stress zones. This results in the generation of a lateral stress beneath the mountains and basins, directed from the basins and foothills toward the mountain range (Zhang & Zhang, 2024c, 2025a). Consequently, the melt generated in the mantle and asthenosphere is subjected to two primary forces: one is the lateral stress (F_x) directed from the basins and foothills toward the mountain core, resulting from the arch tectonic effect; the other is the vertical upward buoyancy (F_y). Under the combined action of these two forces ($F = F_x + F_y$), the melt ascends from the mantle and asthenosphere at a certain angle and converges beneath the interior of the mountain range (as shown in **Figure 3**).

Consequently, significant amounts of melt accumulate in the mantle regions beneath mid-ocean ridges, island arcs, and continental orogenic belts, which ex-

hibit arched tectonic features. At mid-ocean ridges, because the oceanic crust is relatively thin, once magma accumulates beneath the ridge to form a magma chamber, it can easily penetrate the oceanic crust and erupt. In continental orogenic belts, because the continental crust is thicker, once magma enters the crust along faults or fractures, its temperature drops significantly. Some mafic minerals crystallize and precipitate in the lower crust, leaving behind low-temperature, high-viscosity acidic magma that continues to rise, intruding into the overlying rock layers, leading to the uplift of rock strata and the growth of mountain ranges.

Previous studies have proposed various models for magma extraction and convergence beneath mid-ocean ridges and continental orogenic belts, such as ridge suction (Sim et al., 2020), lower crustal flow (Clark & Royden, 2000), and mantle winds (Cao et al., 2026). However, these models not only fail to clarify the origin of magma but also generally suffer from unclear dynamic mechanisms. For instance, the Yellowstone Caldera has experienced repeated eruptions. New geophysical investigations indicate that the magma from these eruptions originates from the asthenosphere, with the initial magma source covering a vast area—spanning thousands of kilometers in width (Farrell et al., 2014)—and potentially extending to the asthenosphere beneath the Eastern Plains (Cao et al., 2026). The driving mechanisms underlying this oblique, cross-lithospheric magma migration have long remained unclear. Cao et al. (2026) suggest that magma migration in the Yellowstone volcano is primarily controlled by lithospheric tectonics, attributing this tectonic control to the interaction between an eastward-directed mantle wind and westward tensional forces within the lithosphere. However, the existence of both the mantle wind and westward tensional stresses within the lithosphere requires further investigation. In fact, the Cordilleran mountain system, where Yellowstone National Park is located, together with the Pacific Ocean to the west and the Great Plains to the east, forms a typical arch-shaped structure. Yellowstone National Park is situated in the "belly" of this arch, a low-stress zone. Magma from the oceanic mantle to the west and the continental mantle of the Great Plains to the east converges upward into the low-stress Yellowstone area; the mechanical mechanism is very clear and requires no additional driving forces. In their geophysical investigations of the crust and mantle beneath the Arxan volcanic group, Han et al. (2018) discovered that magma migrates from the mantle to the crust along an "arch-bridge pattern." The two low points at the base of the arch are located in the Songliao Basin and the Hailar Basin, respectively, while the arch itself is formed by the Greater Khingan Range volcanic group. This "arch-bridge" pathway for magma represents the projection of magma migration under the influence of forces.

3.5. Existing Issues

Currently, the new theory regarding neutrino oscillation-induced radioactive decay and magma formation remains a theoretical hypothesis proposed by only a few scholars and has not yet been reliably verified experimentally. Consequently,

the methodology presented in this paper still involves uncertainties, and the conclusions drawn require further experimental validation. Furthermore, since the time scale of neutrino oscillation (flavor conversion) cannot be determined, the precise value of the minimum resonance width defined in this paper cannot be derived theoretically. Consequently, the arguments presented here are limited to qualitative descriptions and lack quantitative calculations.

4. Conclusion

MSW resonance can excite unstable radionuclides in a medium, accelerating their decay. The molten material inside the Earth is produced by the heat generated from the decay of radionuclides, which is caused by MSW resonance disturbances resulting from atmospheric neutrino oscillations, leading to the melting of some of the material.

The necessary conditions for atmospheric neutrinos to generate MSW resonance within the Earth are: a constant density of the rock layers and a thickness exceeding a certain threshold (d_p). The density of the Earth's crust varies complexly and does not meet the conditions for MSW resonance. In contrast, the mantle is plastic; within relatively thin layers of material, its density remains essentially constant, allowing for the formation of MSW resonance. Therefore, radioactive materials in the crust are not disturbed by MSW resonance and do not produce melt, whereas radioactive materials in the mantle can undergo accelerated decay and generate heat under the disturbance of MSW resonance, thereby producing melt. Since the continental mantle is deeper, the pressure is higher, and the melting point of materials is higher, the same amount of heat melts a smaller volume of continental mantle material compared to the oceanic mantle. Consequently, the amount of melt formed in the continental mantle is far less than that in the oceanic mantle.

Melt generated in the upper mantle is subject not only to upward buoyancy but also to lateral stress directed from basins toward mountain ranges, resulting from the arched tectonic structure of surface mountain ranges. This causes the melt beneath basins to typically converge beneath mountain ranges (including mid-ocean ridges, island arcs, and orogenic belts), leading to higher concentrations of melt beneath mountain ranges than beneath basins (or plains).

The conclusions of this paper are based on a theoretical hypothesis and are subject to a degree of uncertainty; therefore, they require further experimental verification.

Conflicts of Interest

The authors declare no conflicts of interest regarding the publication of this paper.

References

Cao, Z., Liu, L., Wan, B., Chen, L., & Lundstrom, C. (2026). Tectonic Origin of Yellowstone's Translithospheric Magma Plumbing System. *Science, 392,* eady2027.

https://doi.org/10.1126/science.ady2027

Chantel, J., Manthilake, G., Andrault, D., Novella, D., Yu, T., & Wang, Y. (2016). Experimental Evidence Supports Mantle Partial Melting in the Asthenosphere. *Science Advances, 2,* e1600246. https://doi.org/10.1126/sciadv.1600246

Chen, Z. G. (2013). The Earth Expansion Generated the Asthenosphere and Its Formation Time. *Advance in Earth Sciences, 28,* 834-846. (In Chinese)

Choi, C. (2013). Mantle Plumes. *Proceedings of the National Academy of Sciences of the United States of America, 110,* 2435-2435. https://doi.org/10.1073/pnas.1300192110

Chu, W., Xu, Y., Duan, J. X. et al. (2021). Review on the Structure and Density Distribution Characteristics of the Earth's Interior. *Progress in Geophysics, 36,* 443-457. (In Chinese)

Clark, M. M., & Royden, L. H. (2000). *Geology, 28,* 703-706. https://doi.org/10.1130/0091-7613(2000)028<0703:tobtem>2.3.co;2

de Holanda, P. C., Liao, W., & Smirnov, A. Y. (2004). Toward Precision Measurements in Solar Neutrinos. *Nuclear Physics B, 702,* 307-332. https://doi.org/10.1016/j.nuclphysb.2004.09.027

Debayle, E., Bodin, T., Durand, S., & Ricard, Y. (2020). Seismic Evidence for Partial Melt Below Tectonic Plates. *Nature, 586,* 555-559. https://doi.org/10.1038/s41586-020-2809-4

Du, L. T. (2005). Significance of Earth Degassing and Its Research Progress. *Geological Review, 51,* 174-180. (In Chinese)

Dziewonski, A. M., & Anderson, D. L. (1981). Preliminary Reference Earth Model. *Physics of the Earth and Planetary Interiors, 25,* 297-356. https://doi.org/10.1016/0031-9201(81)90046-7

Fang, J., & Xu, H. Z. (1999). Three Dimensional Distribution of Lithospheric Density Beneath the China and Its Adjacent Region. *Progress in Geophysics, 14,* 88-93. (In Chinese)

Farrell, J., Smith, R. B., Husen, S., & Diehl, T. (2014). Tomography from 26 Years of Seismicity Revealing That the Spatial Extent of the Yellowstone Crustal Magma Reservoir Extends Well Beyond the Yellowstone Caldera. *Geophysical Research Letters, 41,* 3068-3073. https://doi.org/10.1002/2014gl059588

Fermi, E. (1934). Versuch einer Theorie der β-Strahlen. I. *Zeitschrift für Physik, 88,* 161-177. https://doi.org/10.1007/bf01351864

Fischer, K. M., Ford, H. A., Abt, D. L., & Rychert, C. A. (2010). The Lithosphere-Asthenosphere Boundary. *Annual Review of Earth and Planetary Sciences, 38,* 551-575. https://doi.org/10.1146/annurev-earth-040809-152438

Gaisser, T. K., & Honda, M. (2002). Flux of Atmospheric Neutrinos. *Annual Review of Nuclear and Particle Science, 52,* 153-199. https://doi.org/10.1146/annurev.nucl.52.050102.090645

Gu, Z. J., Sun, T. Z., & Tao, J. L. (2001). Experiment of Wet Peridotite under High Temperature-Pressure and Asthenosphere Genesis. *Progress in Geophysics, 16,* 40-46. (In Chinese)

Gurney, R. W., & Condon, E. U. (1991). Quantum Mechanics and Radioactive Disintegration. In A. O. Barut, H. Odabasi, & A. van der Merwe (Eds.), *Selected Scientific Papers of E.U. Condon* (pp. 77-92). Springer. https://doi.org/10.1007/978-1-4613-9083-1_11

Han, J. T., Wang, T. Q., Liu, W. Y., et al. (2018). Deep "Arch Bridge" Magmatic System of the Aershan Volcanic Group and Its Stability Analysis. *Seismology and Geology, 40,* 590-610. (In Chinese)

Honda, M., Kajita, T., Kasahara, K., & Midorikawa, S. (1995). Calculation of the Flux of

Atmospheric Neutrinos. *Physical Review D, 52,* 4985-5005. https://doi.org/10.1103/physrevd.52.4985

Hua, J., Fischer, K. M., Becker, T. W., Gazel, E., & Hirth, G. (2023). Asthenospheric Low-Velocity Zone Consistent with Globally Prevalent Partial Melting. *Nature Geoscience, 16,* 175-181. https://doi.org/10.1038/s41561-022-01116-9

Kajita, T. (2010). Atmospheric Neutrinos and Discovery of Neutrino Oscillations. *Proceedings of the Japan Academy, Series B, 86,* 303-321. https://doi.org/10.2183/pjab.86.303

Karato, S. (2012). On the Origin of the Asthenosphere. *Earth and Planetary Science Letters, 321,* 95-103. https://doi.org/10.1016/j.epsl.2012.01.001

Koppers, A. A. P., Becker, T. W., Jackson, M. G., Konrad, K., Müller, R. D., Romanowicz, B. et al. (2021). Mantle Plumes and Their Role in Earth Processes. *Nature Reviews Earth & Environment, 2,* 382-401. https://doi.org/10.1038/s43017-021-00168-6

Lambert, I. B., & Wyllie, P. J. (1970). Melting in the Deep Crust and Upper Mantle and the Nature of the Low Velocity Layer. *Physics of the Earth and Planetary Interiors, 3,* 316-322. https://doi.org/10.1016/0031-9201(70)90068-3

Liu, H., & Yang, X. (2024). The Conductance Effect of Melt in the Upper Mantle and Origin of High Conductivity Anomalies in the Asthenosphere. *Bulletin of Mineralogy, Petrology and Geochemistry, 43,* 1182-1195. https://doi.org/10.3724/j.issn.1007-2802.20240095

Liu, J. H. (2020). Mineralogy and Geological Significance of the Melting Zone in the Jiaohe upper Mantle Fragment, Jilin. *Earth Science Frontiers, 27,* 48-60. (In Chinese)

Lunardini, C., & Smirnov, A. Y. (2000). The Minimum Width Condition for Neutrino Conversion in Matter. *Nuclear Physics B, 583,* 260-290. https://doi.org/10.1016/s0550-3213(00)00341-2

Mao, X. P., Lu-Xu, L. H., Wang, X. M. et al. (2020). Role of Circumferential-Direction Stress in Crustal Movement. *Earth Science Frontiers, 27,* 221-233. (In Chinese)

Mierdel, K., Keppler, H., Smyth, J. R., & Langenhorst, F. (2007). Water Solubility in Aluminous Orthopyroxene and the Origin of Earth's Asthenosphere. *Science, 315,* 364-368. https://doi.org/10.1126/science.1135422

Mikheyev, S. P., & Smirnov, A. Y. (1986). Resonant Amplification of N Oscillations in Matter and Solar-Neutrino Spectroscopy. *Il Nuovo Cimento C, 9,* 17-26. https://doi.org/10.1007/bf02508049

Mikheyev, S. P., & Smirnov, A. Y. (1989). Resonant Neutrino Oscillations in Matter. *Progress in Particle and Nuclear Physics, 23,* 41-136. https://doi.org/10.1016/0146-6410(89)90008-2

Niu, Y. (2023). Geological Confirmation for Water-Effected Incipient Melt Origin of Seismic Low Velocity Zone (LVZ) beneath Ocean Basins. *Science Bulletin, 68,* 359-363. https://doi.org/10.1016/j.scib.2023.01.025

Schmerr, N. (2012). The Gutenberg Discontinuity: Melt at the Lithosphere-Asthenosphere Boundary. *Science, 335,* 1480-1483. https://doi.org/10.1126/science.1215433

Selway, K., & O'Donnell, J. P. (2019). A Small, Unextractable Melt Fraction as the Cause for the Low Velocity Zone. *Earth and Planetary Science Letters, 517,* 117-124. https://doi.org/10.1016/j.epsl.2019.04.012

Sim, S. J., Spiegelman, M., Stegman, D. R., & Wilson, C. (2020). The Influence of Spreading Rate and Permeability on Melt Focusing Beneath Mid-Ocean Ridges. *Physics of the Earth and Planetary Interiors, 304,* Article ID: 106486. https://doi.org/10.1016/j.pepi.2020.106486

Sleep, N. H. (2005). Evolution of the Continental Lithosphere. *Annual Review of Earth and*

Planetary Sciences, 33, 369-393.
https://doi.org/10.1146/annurev.earth.33.092203.122643

Smirnov, A. Y. (2005). The MSW Effect and Matter Effects in Neutrino Oscillations. *Physica Scripta, 121,* 57-64. https://doi.org/10.1088/0031-8949/2005/t121/008

Smye, A. J., & Kelemen, P. B. (2025). Ultra-Hot Origins of Stable Continents. *Nature Geoscience, 18,* 1296-1302. https://doi.org/10.1038/s41561-025-01820-2

The KamLAND Collaboration (2011). Partial Radiogenic Heat Model for Earth Revealed by Geoneutrino Measurements. *Nature Geoscience, 4,* 647-651.
https://doi.org/10.1038/ngeo1205

Upadhyay, A. K., Kumar, A., Agarwalla, S. K., & Dighe, A. (2023). Locating the Core-Mantle Boundary Using Oscillations of Atmospheric Neutrinos. *Journal of High Energy Physics, 2023,* Article No. 68. https://doi.org/10.1007/jhep04(2023)068

Wolfenstein, L. (1978). Neutrino Oscillations in Matter. *Physical Review D, 17,* 2369-2374.
https://doi.org/10.1103/physrevd.17.2369

Xia, Q., Liu, J., Zhang, B., Li, P., Gu, X., & Chen, H. (2022). Water and Partial Melting in the Earth's Mantle. *Acta Petrologica Sinica, 38,* 3631-3646.
https://doi.org/10.18654/1000-0569/2022.12.04

Zhang, G. W. (1999). *The Neutrino Earth Evolution Theory.* Wuhan University of Surveying and Mapping Technology Press.

Zhang, G. W., & Zhang, M. K. (2024a). Research on Neutrino Oscillation-Induced Radioactive Decay. *Modern Physics, 14,* 135-144.
https://doi.org/10.12677/mp.2024.144016

Zhang, G. W., & Zhang, M. K. (2024b). Effects of Matter in Atmospheric Neutrino Oscillations and the Formation of Magma. *Journal of Geoscience and Environment Protection, 12,* 270-287. https://doi.org/10.4236/gep.2024.1212017

Zhang, G. W., & Zhang, M. K. (2024c). Dynamics Model of Arch Structure for Basin-Mountain Evolution. *Gansu Geology, 33,* 1-6. (In Chinese)

Zhang, G. W., & Zhang, M. K. (2026). Matter Effects in Atmospheric Neutrino Oscillations and Radon Anomalies. *Environment and Pollution, 15,* 1-12.
https://doi.org/10.5539/ep.v15n2p1

Zhang, J. B., Liu, Y. S., Foley, S. F., Moynier, F., Zhao, L., Xu, R. et al. (2024). Widespread Two-Layered Melt Structure in the Asthenosphere. *Nature Geoscience, 17,* 472-477.
https://doi.org/10.1038/s41561-024-01433-1

Zhang, M. K., & Zhang, G. W. (2025a). Dynamical Mechanisms of Melt Migration beneath Mid-Ocean Ridges. *Open Journal of Geology, 15,* 358-376.
https://doi.org/10.4236/ojg.2025.157018

Zhang, M. K., & Zhang, G. W. (2025b). Mechanisms for the Formation of Metamorphic Temperature and Pressure Gradients in Orogenic Belts. *Journal of Geoscience and Environment Protection, 13,* 85-101. https://doi.org/10.4236/gep.2025.138005

Zhang, M. K., & Zhang, G. W. (2025c). Neutrino Oscillation, Radioactive Decay, Magmatic Activity and Earthquake Formation. *Open Journal of Earthquake Research, 14,* 172-193.
https://doi.org/10.4236/ojer.2025.144011

Zohoori, D. L., & Spetzler, H. (1970). Partial Melting and the Low-Velocity Zone. *Physics of the Earth and Planetary Interiors, 4,* 62-64.
https://doi.org/10.1016/0031-9201(70)90030-0